grown in mouse erythrocytes in the presence and absence of a few antimalarial drugs. Introduction of a drug causes significant changes in the spectrum of the parasites. The red band is broadened and centered around 640 nm, the Soret band is blue-shifted from 400 to 375 nm or lower, and the I_S/I_r ratio increases significantly. The Soret band shifts indicate FP-drug interaction, while the increase in the intensity ratio points to a reduction in the population of FP self-aggregates on drug addition. In previous studies (*15, 17*), we showed that FP can form a 2:1 molar complex with chloroquine in aqueous solution with a formation constant that appears comparable to the binding of chloroquine to hemin and to parasite suspensions (*18*). We thus believe that our present results provide the first direct evidence for the presence of FP and drug complex in malarial parasites (*19*).

It also appears that the photoacoustic method can readily distinguish between chloroquine-sensitive and -resistant strains of *P. chabaudi* (Fig. 1). Unlike the drug-sensitive strain, the resistant one displays the Soret maximum at about 430 nm and a reduced I_S/I_r ratio of 1.30. The ratio is close to the values of 1.4 and 1.5 seen in the photoacoustic spectrum of hemoglobin (*10*), while the position of the Soret band is similar to that seen in the optical spectra of heme coordinated to a peptide chain, for example, hemoglobin and its derivatives (*20*). Hence, it appears that endogenous FP in the resistant parasite is largely in the form coordinated to a protein chain. It is known that when *P. berghei* becomes resistant to chloroquine, production of the pigment drops (*21*). Fitch and Chevli (*22*) argued that the molecular change responsible for chloroquine resistance could involve either hemoglobin degradation or FP sequestration. In light of our results, it appears likely that drug resistance, at least in *P. chabaudi*, involves the former process in such a way that the degradation of hemoglobin occurs to a stage where the heme group is still held to the peptide chain with the same integrity as in the whole molecule (*23*).

The form of the endogenous FP that complexes with drugs is still not known. Neither the pigment nor aged self-aggregate of FP (*14*) appear to be membranelytic, and free FP, which does lyse membranes, is not detected in the parasite. It is reasonable to conceive of the endogenous FP as being in a state of equilibrium; from this FP the added drug derives its partner to form the lytic complex (Fig. 3). Since the complex can be isolated as a heteromolecular aggregate species (*18, 24*), drug interaction with the FP self-aggregates is a possibility. Drugs do not seem to bind to the pigment (*11*) or to residual hemoglobin (*18*), although they do bind to protease-degraded fragments of hemoglobin (*15*). We propose the scheme shown in Fig. 3 as a model of the mode of action of quinoline drugs on the malaria parasite.

D. BALASUBRAMANIAN*
CH. MOHAN RAO
Centre for Cellular & Molecular Biology, Regional Research Laboratory Campus, Hyderabad 500 007, India
B. PANIJPAN
Department of Biochemistry, Faculty of Science, Mahidol University, Bangkok 10400, Thailand

References and Notes

1. K. A. Yamada and I. W. Sherman, *Exp. Parasitol.* **48**, 61 (1979).
2. A. U. Orjih, H. S. Banyal, R. Chevli, C. D. Fitch, *Science* **214**, 667 (1981).
3. Y. Inada and K. Shibata, *Biochem. Biophys. Res. Commun.* **9**, 323 (1962).
4. W. I. White, in *The Porphyrins*, D. Dolphin, Ed. (Academic Press, New York, 1978), vol. 5, p. 303.
5. G. H. Beaven, S. H. Chen, A. D'Albis, W. B. Gratzer, *Eur. J. Biochem.* **41**, 539 (1974).
6. E. Tipping, B. Ketterer, L. Christodoulides, G. Enderby, *Biochem. J.* **157**, 461 (1976).
7. T. A. Moore, *Photochem. Photobiol. Rev.* **7**, 187 (1983).
8. D. Balasubramanian and Ch. Mohan Rao, *Photochem. Photobiol.* **34**, 749 (1981); D. Balasubramanian, *Biosci. Rep.* **3**, 981 (1983).
9. D. Cahen, G. Bults, H. Garty, S. Malkin, *J. Biochem. Biophys. Methods* **3**, 293 (1980).
10. A. Rosencwaig, *Photoacoustics and Photoacoustic Spectroscopy* (Wiley, New York, 1980).
11. W. Sirawaraporn, B. Panijpan, Y. Yuthavong, *Exp. Parasitol.* **54**, 262 (1982).
12. P. A. Kramer and J. E. Matusik, *Biochem. Pharmacol.* **20**, 1619 (1971); D. F. H. Wallach and M. Conley, *J. Mol. Med.* **2**, 119 (1977).
13. C. A. Appleby, N. A. Nicola, J. G. R. Hurrel, S. J. Leach, *Biochemistry* **14**, 4444 (1975).
14. The suggestion of endogenous FP self-aggregates prompted us to study their ability to lyse red blood cells. We found the hemolysis efficiency of aggregates of hemin aged for 3 to 5 hours at 37°C to be extremely low. The rate was enhanced somewhat by the addition of chloroquine.
15. A. Jearnpipatkul, P. Govitrapong, Y. Yuthavong, B. Panijpan, *Experientia* **36**, 1063 (1980); A. Jearnpipatkul and B. Panijpan, *Chem. Biol. Interact.* **33**, 83 (1980); W. Peters and R. W. Howells, in *Rodent Malaria*, R. Killick-Hendericks and W. Peters, Eds. (Academic Press, London, 1978), p. 169.
16. C. A. Homewood *et al.*, *Ann. Trop. Med. Parasitol.* **69**, 283 (1975); C. A. Homewood, J. M. Jewsbury, M. L. Chance, *Comp. Biochem. Physiol. B* **43**, 517 (1972).
17. B. Panijpan, Ch. Mohan Rao, D. Balasubramanian, *Biosci. Rep.*, in press.
18. A. C. Chou, R. Chevli, C. D. Fitch, *Biochemistry* **19**, 1543 (1980).
19. The drug-induced photoacoustic spectral changes are better reflected when a higher modulation frequency (912 Hz) is used, implying that a significant fraction of the absorbing species might lie closer to the surface (*10, 11*). This, however, is not a foolproof interpretation, since the lyophilized and diluted samples of the parasites need not be all intact.
20. M. A. Waterman, *Methods Enzymol.* **52**, 456 (1978).
21. R. Ladda and H. Sprinz, *Proc. Soc. Exp. Biol. Med.* **130**, 524 (1969).
22. C. D. Fitch and R. Chevli, *Antimicrob. Agents Chemother.* **19**, 589 (1981).
23. That photoacoustic spectroscopy can distinguish chloroquine-resistant parasites from sensitive ones suggests that it might be possible to monitor infected erythrocytes or blood smears directly by this method and, after suitable correction for background hemoglobin signals, to check whether the parasites are drug-sensitive or not.
24. G. Blauer and H. Ginzburg, *Biochem. Int.* **5**, 519 (1982).
25. Ch.M.R. is a senior research fellow of the Council for Scientific and Industrial Research, India. B.P. was aided by a grant from the United Nations/World Bank/World Health Organization Special Programme for Research and Training in Tropical Diseases. We are grateful to the University of Hyderabad for access to their photoacoustic instrument and to D. Walliker for cloned strains of *P. chabaudi*.
* Address correspondence to D.B.

10 August 1983; accepted 30 November 1983

An Ultrahigh-Speed Analysis of Exocytosis: Nematocyst Discharge

Abstract. *High-speed microcinematography of nematocyst discharge in* Hydra attenuata *Pall. shows that this specialized exocytosis, which appears to result from an increase in the intracapsular pressure, requires a total of about 3 milliseconds. A maximum velocity of 2 meters per second is generated, corresponding to an acceleration of 40,000g. Thus nematocyst discharge is one of the fastest cellular processes in nature.*

The nematocytes (cnidocytes or "stinging cells") of the *Cnidaria* serve various functions such as capture of prey, defense, and locomotion. The essential organelle of these cells, the capsular nematocyst, is an extremely complex secretory product of the Golgi apparatus (*1*). When triggered, it ejects its tubular content by evagination (*2, 3*). Three hypothetical mechanisms have been suggested for this exocytosis (*4*): (i) discharge is caused by a swelling of the capsular matrix due to an influx of water [osmotic hypothesis (*5*)]; (ii) intrinsic tension forces generated during cnidogenesis are released at discharge [tension hypothesis (*6*)]; or (iii) contractile units enveloping the cyst cause the discharge when they increase the cyst's internal pressure by deformation of its wall [contractile hypothesis (*5*)].

We have studied the discharge of stenotele cysts (Fig. 1) in *Hydra attenuata* Pall. (Hydrozoa). This process is normally triggered mechanically by a prey (usually a small crustacean). The cyst everts three stylets (Fig. 1), which join to form an arrowhead that punches a hole

into the prey's integument. In a second step a long (470 ± 77 μm) and slender (diameter, 0.8 ± 0.11 μm) tubule evaginates (*3*) through this opening into the prey's body and releases toxins that paralyze and kill the prey.

We have analyzed this process by means of ultrahigh-speed microcinematography. For technical reasons the cinematographical analysis was performed on freely exploding stenoteles. Isolated live tentacles of *Hydra* were placed on a microscopic slide onto which two electrodes had been mounted (*7*); cysts were triggered by an electrical pulse (30 μsec, 24 Vd.c.), which was synchronized with the high-speed camera (*8*) and observed with bright-field optics. A total of 20 individual discharges were filmed (see Fig. 2).

Analysis of the films shows that the entire discharge process [from the flipping open of the operculum to tubule evagination (*9*)] is completed in about 3 msec. It can be subdivided into four phases (Fig. 3).

Phase a: During the interval between the onset of the electrical stimulus and the flipping open of the operculum of the cyst (*10*), the cyst volume undergoes a 10 percent increase (Fig. 4), which is the first visible reaction of the capsule to the stimulus.

Phase b: The capsule's cover is opened and the stylet-bearing portion of the tubule ejected. In one film, images of both the undischarged cyst and the cyst with ejected stylets appeared on the same frame. Since the exposure time (*11*) per frame is 10 μsec (the shutter closes for 15 μsec between frames), the second phase must be completed in considerably less than 10 μsec. The stylet tip must travel a distance of approximately 20 μm during this period, giving an average velocity (*12*) of 2 m sec^{-1}. A constant acceleration (*12*) of 4×10^5 m sec^{-2} or about 40,000*g* is required to produce this average velocity over a 10-μsec period from a standing start.

Phase c: The discharge is temporarily arrested for approximately 150 μsec (Fig. 3). During this period, the stylets must withdraw from the opening they have created mechanically (*13*) in order that the rest of the tubule may evaginate into the prey's body. In numerous scanning electron microscope pictures of discharged stenoteles, stylets are always flipped back clear of the hole (*3*).

Phase d: The conical part of the tubule, bearing the three rows of lamellae (Fig. 1), and the long terminal part of the tubule are evaginated. This process is completed when the last portions of the tubule have disappeared from the inside of the capsule. This phase is the slowest of all and is variable (Fig. 3). The evagination of the longest section of the tubule occurs at a velocity of about 0.3 m sec^{-1}, considerably slower than that of the ejection of the stylets (phase b).

Earlier measurements (*3*) have revealed that the stenotele capsule loses 50 percent of its volume during complete discharge (*14*). Our measurements show that this change is stepwise (Fig. 4). It is preceded by a slight but distinct increase in volume (10 percent) immediately before the ejection of the stylets. In phase b there is a rapid decrease to 75 percent of the resting volume; this is followed by a slower but steady decrease to 50 percent of the original volume in phases c and d.

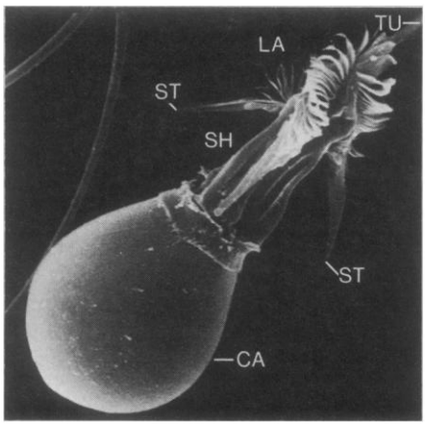

Fig. 1. Scanning electron micrograph (×2600) of a discharged stenotele; *CA*, capsule; *LA*, lamellae; *SH*, shaft; *ST*, stylet; *TU*, tubule.

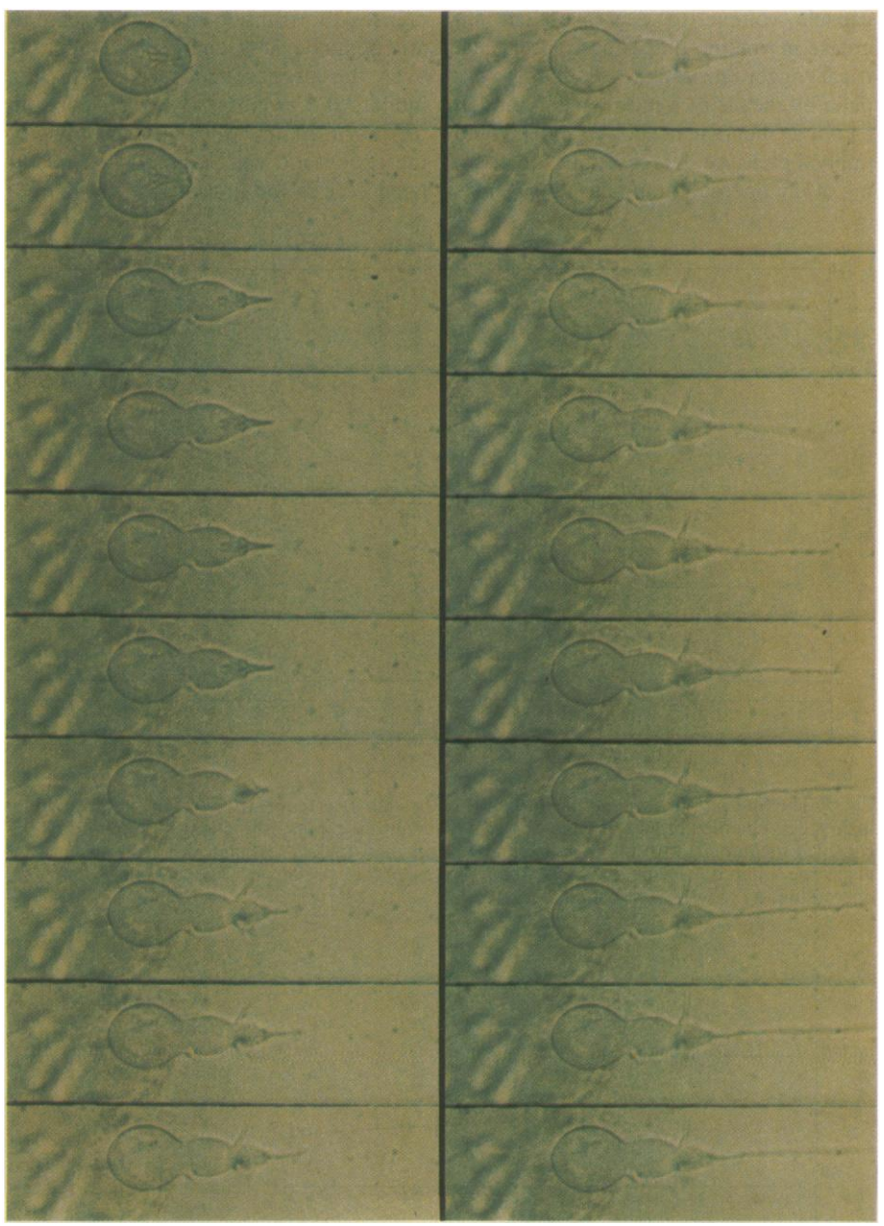

Fig. 2. Cinematographically recorded sequences of stenotele discharge, including phases a, b, c, and d [direct copy of original film, 40,000 frames per second, bright-field optics (×1000)].

Throughout these volumetric changes, the cyst retains its typical shape and shows no signs of deformation.

The volume decrease is consistent with the contractile hypothesis (*15*), but one can calculate from the volume decrease in phase b that the surface area must shrink by 22 percent in a period of less than 10 μsec. If this change were caused by contracting filaments, they would have to shorten by 11 percent in this period (11,000 lengths per second); this is about 500 to 1000 times faster than in the fastest known striated muscles (*16*). Staining of nematocytes with fluorescent phalloidine has failed to show the existence of organized bundles of actin filaments in the immediate neighborhood of the cyst (*17*).

A purely osmotic discharge mechanism would not lead one to expect the capsule volume to decrease. The increase in volume that is seen after electrical triggering, however, is hard to explain by means of a pure tension model; a volume increase in such a model would imply a pressure decrease, but the opening of the operculum in phase b suggests a pressure increase. We therefore propose that in stenotele discharge the initial volume increase is produced osmotically, whereas the subsequent discharge involves in addition the release of mechanical energy stored in the capsular wall. We envision that a substantial portion of the mechanical energy is released during the rapid ejection of the stylets (phase b), while pressure created by the swelling of the osmotically active capsular matrix is the main driving force of the subsequent, slower events (phases c and d).

Our observations raise questions about the molecular basis of the postulated forces, especially of the internal pressure of the nematocyst, before and during discharge. It has been shown (*18*) that in sea anemones (Anthozoa) the removal of intracapsular calcium increases the osmotic pressure and initiates nematocyst discharge in vitro. However, the mechanism by which calcium inhibits the swelling of the cyst is still unknown. In other systems a swelling of the exocytotic vesicles has been postulated (*19*) as the first step in discharge. Nematocyst discharge may therefore serve as a model for the understanding of other exocytotic processes and biophysical problems related to them.

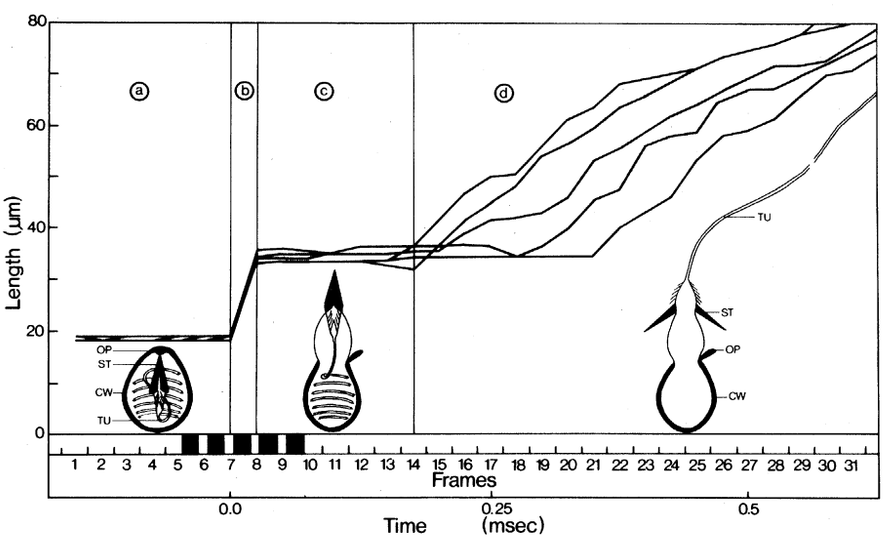

Fig. 3. The four phases of stenotele discharge (a through d) as reconstructed from five individual high-speed cinematographical runs (Fig. 2). The curves express the changes in length of the capsules including those of their evaginated contents (stylets, tubule) along the process of discharge (that is, during the four main phases of the process). *CW*, capsular wall; *OP*, operculum; *ST*, stylet; *TU*, tubulus.

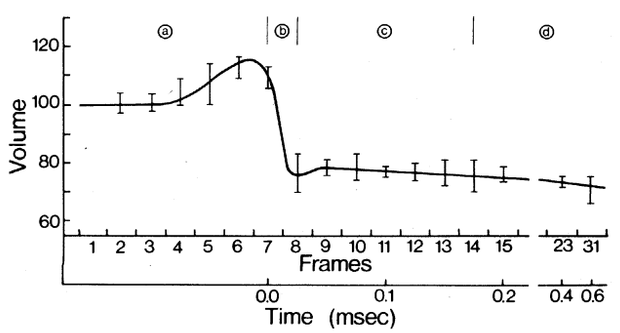

Fig. 4. Average values ($N = 5$) of the volumetric changes (expressed as a percentage of the initial volume) of the stenotele capsule after triggering and during the process of discharge (Fig. 3). The volume of the spherical capsule is calculated according to the procedures of Tardent and Holstein (*3*).

T. Holstein*
P. Tardent

Department of Zoology,
University of Zürich-Irchel,
CH-8057 Zürich, Switzerland

References and Notes

1. T. Holstein, *J. Ultrastruct. Res.* **36**, 276 (1981).
2. P. Tardent, T. Honegger, R. Baenninger, in *Developmental and Cellular Biology of Coelenterates*, P. Tardent and R. Tardent, Eds. (Elsevier–North Holland, Amsterdam, 1980), p. 331.
3. P. Tardent and T. Holstein, *Cell Tissue Res.* **224**, 269 (1982).
4. The term "exocytosis" is used for nematocyst discharge, although it is still not known whether the behavior of the membranes corresponds to that of a classical exocytosis.
5. R. N. Mariscal, in *Coelenterate Biology*, L. Muscatine and H. M. Lenhoff, Eds. (Academic Press, New York, 1974), p. 129.
6. D. Carré, *Eur. J. Cell Biol.* **2**, 265 (1980).
7. We mounted the electrodes on the slide at a distance of 10 mm by evaporating the surface of the slide with chromium (~ 150 Å), palladium (~ 150 Å), and gold (~ 200 Å). They were reinforced by galvanization with a ~ 30-μm layer of elemental gold.
8. The Zeiss Universal microscope was equipped with an 63/1.4 oil planapochromate lens and a 1.4 condenser system. A Hycam 16 mm/120 m high-speed camera (Redlake City Corporation) was coupled with the microscope by means of a microscope-projective optic 125 mm and a Zeiss cine adapter. The camera was fitted with an optical head for 1/4 frame 16 mm, a timing light and zero mark block, and a rotary shutter for 1/4 frame 1:2.5). The source of light was a 75-W xenon lamp (luminous density, 40,000 candela cm^{-2}) supplied with a Siemens VHXC 75/100. Electrical triggering of nematocyst discharge was synchronized with the high-speed camera through a Cu-6a control unit and a PR 4a programmer (Weinberger, Zürich). Kodak Ektachrome VNF 7250 (400 ASA, tungsten) was used. Film analysis was performed with a Vanguard M 16 C motion analyzer equipped with an HP 9874 a digitizer and an HP 9845 b computer.
9. Since the tip of the long evaginating tubule always went out of the optic range, the end of the process was timed when the inside of the capsule was clear of the tubule.
10. The delay between the onset of the electrical stimulus and the initiation of cyst discharge varies between 0.025 and 2.5 msec. This variation most likely results from variation in the time required for the contacts of the relay (in the CU-6a control unit) to close. Only cysts of functional nematocytes (mounted in the battery cell) can be electrically stimulated. Therefore, we assume that discharge after electrical stimulation is representative of a normal situation.
11. Exposure time was $t_e = p \cdot f_B^{-1}$ (p is the shutter ratio, that is, the ratio of the "open-position" of the camera shutter referred to the total disk of 360°; f_B is the number of frames per second).
12. Velocity of the stylet tips = $v = s \cdot t^{-1}$ (t is the time required for the process, and s is the distance the stylets cover). Assuming constant acceleration (a), $s = \int v \cdot dt = \int a \cdot t \cdot dt = 1/2\ a \cdot t^2$. Gravitational acceleration (g) = 9.80665 m sec^{-2}.
13. The contribution of enzymes in perforating cuticular obstacles is most unlikely since the stenoteles of *Hydra attenuata* do not contain chitinase (M. Klug, P. Tardent, J. Smid, T. Holstein, *J. Exp. Zool.*, in press).
14. Nondischarged volume, 1283.6 ± 126.5 μm^3; discharged volume, 652.3 ± 110.3 μm^3.
15. S. M. Cormier and D. A. Hessinger, *Tissue Cell* **12**, 713 (1980).
16. R. Close, *J. Physiol. (London)* **180**, 542 (1965).
17. T. Holstein, unpublished results.
18. R. Lubbock and W. B. Amos, *Nature (London)* **290**, 500 (1981); R. Lubbock, B. L. Gupta, T. A. Hall, *Proc. Natl. Acad. Sci. U.S.A.* **78**, 3624 (1981).
19. H. B. Pollard, C. J. Pazoles, C. E. Creutz, O. Zinder, *Int. Rev. Cytol.* **58**, 159 (1979); M. Bilinski, H. Plattner, H. Matt, *J. Cell Biol.* **88**, 179 (1981).
20. This project was supported by the Swiss National Science Foundation (grant 3.174–0.81) and

the Bundesstaatliche Hauptstelle für wissenschaftliche Kinematographie, Vienna. We thank R. Riedl for his support and W. Völlenkle, W. Ziegler, and H. Herschner for their help in using the high-speed camera. We thank E. Hauschteck, R. Portmann, P. Siegrist, and E. Wenk for technical assistance and advice. We are also indebted to C. N. David and H. K. MacWilliams who offered criticisms of the manuscript.

* Present address: Department of Zoology, University of Munich, Luisenstrasse 14, D-8000 Munich 2, Federal Republic of Germany.

7 November 1983; accepted 30 November 1983

Avian Pancreatic Polypeptide Phase Shifts Hamster Circadian Rhythms When Microinjected into the Suprachiasmatic Region

Abstract. *The suprachiasmatic nucleus has been identified tentatively as a circadian pacemaker. To examine the functional role of peptides found within suprachiasmatic neurons, avian pancreatic polypeptide and vasopressin were microinjected into the suprachiasmatic region. Avian pancreatic polypeptide, but not vasopressin, shifted the phase of the wheelrunning rhythm as a function of the time of its injection within the circadian cycle. Avian pancreatic polypeptide or a similar peptide may be one component of the neurochemical processes underlying entrainment to the light-dark cycle.*

Many of the complex daily patterns in mammalian physiology and behavior are controlled by the circadian timing system. Circadian pacemakers generate precise rhythms in physiological systems that are close to, but rarely, 24 hours (*1*). The synchronization of these endogenous rhythms with the 24-hour light-dark (LD) cycle is achieved by daily resetting of the circadian pacemaker's phase (*2, 3*). Whether light advances or delays the phase depends on the time of the circadian cycle when light exposure occurs.

Neurons of the suprachiasmatic nuclei (SCN) of the hypothalamus have been identified as a putative circadian pacemaker. Destruction of the SCN eliminates the circadian rhythmicity of a large number of behavioral and physiological variables (*4, 5*). The SCN exhibits circadian variations in metabolic activity (*6*) and rhythms in multiple-unit electrical activity, despite surgical isolation from other hypothalamic areas (*7*). The phase resetting of circadian timing that occurs after exposure to brief light pulses can be mimicked by electrical stimulation of the SCN (*8*) or by intraventricular injections of carbachol, a cholinergic agonist (*9*).

Little is known about the physiological mechanisms that mediate the entrainment of SCN neurons to the LD cycle, generate circadian variations in SCN activity, or communicate circadian information to other physiological systems. Anatomical studies, however, have provided much information on the morphology, neurochemistry, and afferent projections of the SCN (*5*). A large population of neurons within the nucleus contain vasopressin (VP), vasoactive intestinal peptide, or somatostatin (*10*). The ventrolateral area of the SCN seems to be the primary terminus of SCN afferents, including a monosynaptic pathway from the retina, the retinohypothalamic tract (*11*). Other well-defined fiber systems that terminate in the ventrolateral SCN include a serotoninergic pathway from the midbrain raphe (*12*) and a secondary visual projection from the ventral region of the lateral geniculate nucleus (vLGN) of the thalamus (*13*) that contains avian pancreatic polypeptide (APP) immunoreactivity (*14*).

We examined the effect of microinjections of APP and VP into the suprachiasmatic region on the circadian rhythm of locomotor activity in the hamster. Adult male hamsters housed in cages containing activity wheels were implanted stereotaxically with guide cannulas aimed at the suprachiasmatic region (*15*). After surgery, each hamster was housed under constant illumination and allowed to establish a stable free-running circadian activity rhythm. At 10- to 14-day intervals the unanesthetized hamsters were removed from their cages and injected with VP (200 ng) or APP (200 ng) in 200 nl of 0.9 percent NaCl (*16*). All injection sites were verified histologically (*17*).

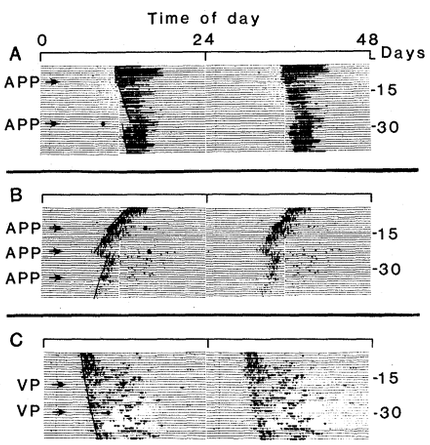

Fig. 1. Effects of avian pancreatic polypeptide (*APP*) and vasopressin (*VP*) microinjected into the suprachiasmatic region on the phase of hamster activity rhythms free-running in constant light. (A and B) Phase-shifts in the activity rhythm produced by microinjection of APP at various phases of the circadian cycle (circles indicate time of injection). (C) Absence of phase shifts in the activity rhythm after microinjection of VP.

Whether microinjection of APP into the suprachiasmatic region advanced or delayed the phase of the activity rhythm depended on the time within the circadian cycle at which it was administered. The shift in the phase of the activity rhythm was fully expressed 1 to 4 days after the injection of peptide (Fig. 1). The data obtained from all APP injections were then plotted in a phase response curve (Fig. 2) that illustrates the magnitude and direction of the phase shifts (*18*) produced by APP injected at various times throughout the circadian cycle. Injection of APP within a 10-hour interval prior to the onset of the wheelrunning [circadian time (CT) 2 through 12] consistently advanced the phase of the activity rhythm. The largest phase advances occurred when APP was administered between CT 6 and CT 10. When injected between 6 and 14 hours after the onset of wheelrunning, APP produced phase delays in the activity rhythm. The delays in the circadian phase, however, were more variable than the phase advances. The transitions between APP-produced phase advances or delays were abrupt, with little indication of a time when animals did not respond to the peptide. Despite the induction of phase shifts in the activity rhythm, the free-running circadian period was not altered after APP injection (-0.05 ± 0.03 hour).

The proximity of the injection site to the third ventricle suggested that APP could have penetrated into the ventricular system and thereby acted on more remote structures. To explore this possibility, we examined the effects of APP injected into the lateral ventricle. Intraventricular administration at times within the circadian cycle that produced maximal phase advances and delays when injected within the suprachiasmatic region had no effect on circadian phase. Injections between CT 6 through 10 and CT 20 through 24 resulted in phase shifts of -0.31 ± 0.22 hour (mean ± standard error, $N = 2$) and $+0.08 \pm 0.19$ hour ($N = 3$), respectively.

Microinjection of VP into the suprachiasmatic region at various times throughout the circadian cycle produced no consistent pattern of phase shifts in the activity rhythm (Fig. 1). The magni-